Journal of Molecular Structure 1068 (2014) 130–139

Contents lists available at ScienceDirect

Journal of Molecular Structure

journal homepage: www.elsevier.com/locate/molstruc

Experimental and theoretical study on the dissociative photoionization of trans-2-methyl-2-butenal

Yuquan Li [a], Maoqi Cao [a], Jun Chen [a], Yanlin Song [a], Xiaobin Shan [a], Yujie Zhao [a], Fuyi Liu [a], Zhenya Wang [b], Liusi Sheng [a,*]

[a] School of Nuclear Science and Technology, National Synchrotron Radiation Laboratory, University of Science and Technology of China, Hefei 230029, China
[b] Laboratory of Environmental Spectroscopy, Anhui Institute of Optics and Fine Mechanics, Chinese Academy of Sciences, Hefei 230031, China

HIGHLIGHTS

- Ionization energy of the molecule is determined.
- Appearance energies of main fragment ions are determined for the first time.
- The mechanism of the dissociation procedure is studied.
- Ring forming and H shift are found in the dissociation of parent ion.

GRAPHICAL ABSTRACT

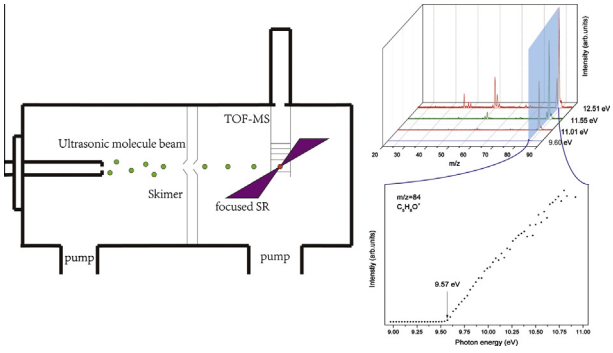

ARTICLE INFO

Article history:
Received 26 November 2013
Received in revised form 8 March 2014
Accepted 13 March 2014
Available online 20 March 2014

Keywords:
Trans-2-methyl-2-butenal
Synchrotron radiation
Dissociative photoionization
Theoretical calculation
CBS-QB3

ABSTRACT

The dissociative photoionization of trans-2-methyl-2-butenal was investigated with photoionization mass spectrometer in photon energy region between 8.97 and 15 eV. The ionization energy (IE) of trans-2-methyl-2-butenal and the appearance energies (AEs) of major fragment ions $C_5H_7O^+$, $C_4H_5O^+$, $C_4H_8^+$, $C_4H_7^+$, $C_3H_5^+$, $C_3H_4^+$, $C_2H_4^+$, CHO^+, $C_2H_4O^+$ and $C_3H_3^+$ are obtained to be 9.57, 10.71, 10.68, 10.59, 11.55, 11.94, 11.82, 12.03, 12.21, 12.09 and 12.90 eV respectively by measurement of the photoionization efficiency curves (PIEs). Based on the experimental results, six major dissociative photoionization channels, $C_5H_7O^+ + H$, $C_4H_5O^+ + CH_3$, $C_5H_6^+ + H_2O$, $C_4H_8^+ + CO$ ($\rightarrow C_3H_5^+ + CH_3 + CO$, $C_3H_4^+ + CH_4 + CO$, $C_2H_4^+ + C_2H_4 + CO$, $C_4H_7^+ + H + CO$), $C_4H_7^+ + CHO$ ($C_4H_7 + CHO^+$), and $C_3H_4 + C_2H_4O^+$ are proposed with the aid of theoretical calculations at the level of CBS-QB3. Both direct dissociation and isomerization of the parent ion exist during the fragment forming procedure. H shift and ring formation are found to be dominant in the isomerization of the parent ion. Transition states and intermediates involved in the dissociation channels are also determined.

Introduction

α,β-Enone, as a group of volatile organic compounds (VOCs), plays an important role in the formation of secondary organic aerosol (SOA) via photooxidation in atmosphere, and trans-2-methyl-2-butenal (t-2M2B) is widely found in the ambient. It is considered to be the oxidation product of the vastly existing unsaturated hydrocarbon: isoprene and other volatile organic compounds from both anthropogenic and biogenic sources [1–7]. Leaf wounding is also a significant source of t-2M2B that enters the environment along with other VOCs [8,9]. It is well known that the aldehydes

* Corresponding author.
E-mail address: lssheng@ustc.edu.cn (L. Sheng).

http://dx.doi.org/10.1016/j.molstruc.2014.03.021
0022-2860/

contributes to the generation of SOA through heterogeneous reactions [10]. Lately, research work done by Chan et al. shows that the SOA mass yields are the highest for aldehydes that are α,β-unsaturated and contain an additional methyl group on the α-carbon [11]. They summarized aerosol yields of 9 VOCs studied by Atkison and Arey [3], Magneron et al. [12], Tuazon et al. [13], and Fantechi et al. [14]. Aerosol yield of t-2M2B rank the second which is slightly lower than the aerosol yield for methancrolein, but at least an order of magnitude higher than that for the other several VOCs. In experiment done by Chan, t-2M2B has a relatively much higher aerosol yield than 3-methyl-2-butenal (3M3B). It is notable that differences in the group on the α-carbon between the two homologues lead to the differences in their aerosol yields. Obviously, information on the molecule structure matters in the study of aerosol formation via atmospheric chemical reaction.

However, works on t-2M2B have been focused on the reaction rate constants with oxidants common in ambient: NOx, OH and O_3 [11,15,16]. Up to now, few works have been done on the structure of t-2M2B molecule itself, only the IE of the molecule is available [17]. Lots of theoretical and experimental works focus on its C3 and C4 homologues: acrolein [18–21] and trans-crotonaldehyde [22]. The H atom and CHO elimination by direct C–C bond cleavage are found to be dominant in their dissociation. To the best of our knowledge no further information on the fragment ions from parent ion of t-2M2B could be available, let alone the mechanism of the dissociation pathways for the fragment ions.

We carried out the experiment of dissociative photoionizaiton of t-2M2B using tunable synchrotron radiation and supersonic molecular beam technique coupled with photoionization mass spectrometry. The mass spectrum at photon energy of 15 eV is obtained. IE of the t-2M2B molecule and AEs for its fragment ions are determined from the photoionizaiton efficiency curves (PIEs). With the aid of theoretical calculations, mechanisms of the dissociation pathways are discussed. In addition, the transition states and the intermediates involved in the pathways are also obtained by theoretical calculations and described in detail in this article. Theoretical outcomes match fairly well with the experimental results. This work provides a better understanding of the fragmentation pathways of trans-2-methyl-2-butenal.

Experimental section

Our experimental work was carried out at National Synchrotron Radiation Laboratory, Hefei, China. The apparatus has been described elsewhere [23–26]. To be brief, a photoionization time-of-flight mass spectrometry (PI-TOF-MS) is affiliated to a supersonic expansion molecule beam system at Atomic and Molecular Physics Beamline. The synchrotron radiation from the undulator of the 800 MeV electron storage ring serves as a "soft" photoionization source here. The radiation is then monochromatized by the monochromator equipped with a grating of 370 lines/mm. It covers the energy range from 7.5 to 22.5 eV [23,25]. To eliminate the high order harmonic generated by the undulator, a rare gas harmonic filter is set right before the photoionization chamber. Ar (IE = 15.759 eV, NIST (National Institute of Standards and Technology)) is selected as the gas filter medium for photon energy $\leqslant$15.7 eV. Former works showed that at photon energy of 12 eV and using N_2 (IE = 15.581 eV) as the sample, the suppression efficiency of the filter is above 99.9% when the pressure of the filter chamber is about 5 Torr [23]. During our experiment, the pressure of filter is kept above 5 Torr.

The trans-2-methyl-2-butenal (CAS: 497-03-0) sample is obtained commercially from J&K CHEMICA. The purity of the sample is above 98%. It is used directly without further purification in our experiment. The sample is sealed in a stainless steel can that was connected to the molecule expansion chamber with a stainless steel pipeline of a diameter of 6 mm. As the sample is volatilizable at normal temperature, no carrying gas is employed. After the sample steam is expanded in the chamber, the supersonic molecular beam is generated and it passes throw two skimmers with diameter of 1 mm before it arrives at the ionization zone. The monochromatized photon is focused on the ionization zone with photon flux of about 10 [12] photons/s. The generated ions are picked up and detected by a multichannel plate (MCP) detector. The signal is amplified with a preamplifier VT120C (EG&G, ORTEC). A multiscaler P7888 counter (FAST Comtec, Germany) counts and transfer the signal to computer. The chamber was pumped to around 1×10^{-5} Pa before and after the experiment and around 1×10^{-3} Pa during the experiment.

The mass spectrum at photon energy of 15 eV is obtained. PIEs of the fragment ions are obtained by scanning the photon energy continuously in steps of 0.03 eV and the TOF mass spectra are collected. To normalize the ion signals simultaneously, the photon intensity is monitored with a silicon photodiode (SXUV-100, International Radiation Detectors, Inc.) during the experiment.

Theoretical methods

All the energies of the neutral molecule, fragment ions, intermediates and transition states are calculated in high level ab initio method CBS-QB3 [27,28]. In CBS-QB3 method, geometries are optimized and frequencies are calculated at the level of B3LYP/6-311G(d, p). Second, energy calculations at MP2/6-311+G(2df, 2p) level are done and CBS extrapolation is calculated. Third, MP4(SDQ)/6-311G(d, p) and QCISD(T)/6-311G(d, p) single point energies are computed. Finally, two empirical correction terms: effect of absolute overlap integral and spin contamination, are considered in the overall energy estimate. The stationary points are identified with frequency calculations at the same level to verify that minima and transition state structures have a zero and only one imaginary frequency, respectively. The intrinsic reaction coordinate (IRC) calculations at the same level with geometry optimization are applied. Some of the direct bond cleavages are also scanned at the same level. All ab initio calculations are performed using the GAUSSIAN 09 [29] suite of program at the supercomputing center of USTC, Hefei, China.

Results and discussion

Results

Photonionization mass spectra of t-2M2B at 15 eV is shown in Fig. 1. In the mass spectra, as no signal at mass greater than that of $C_5H_8O^+$ (m/z = 84) is detected, all the fragments are considered to be originated from parent ion $C_5H_8O^+$. We have also inspected mass spectra at 10.0 and 12.0 eV to ensure that no signal at m/z = 168 (two times of 84) or more is detected. Cluster is not detectable in our experiment. Four major fragment peaks at m/z = 84, 55, 41, and 29 are assigned to be $C_5H_8O^+$, $C_4H_7^+$, $C_3H_5^+$ and CHO^+. Five medium peaks at m/z = 83, 56, 44, 39, 29 and 28 are assigned to be $C_5H_7O^+$, $C_4H_8^+$, $C_2H_4O^+$, $C_3H_3^+$ CHO^+ and $C_2H_4^+$. A group of weak peaks appears at m/z = 71, 69, 66 and 65. Peak at 69 is the product of methyl elimination ($C_4H_5O^+$) and 66 is that of dehydration reaction ($C_5H_7^+$).

Mass spectra obtained at different photon energies are shown in Fig. 2. It indicated that at photon energy of 9.60 eV only parent ion is found and fragments ions emerge gradually as the photon energy increases. The peak of m/z = 55 is not distinguishable until the photon energy is around 11.55 eV. PIEs of fragment ions are shown in Fig. 4(a)–(d). In this article, we apply approach of the PIE curves

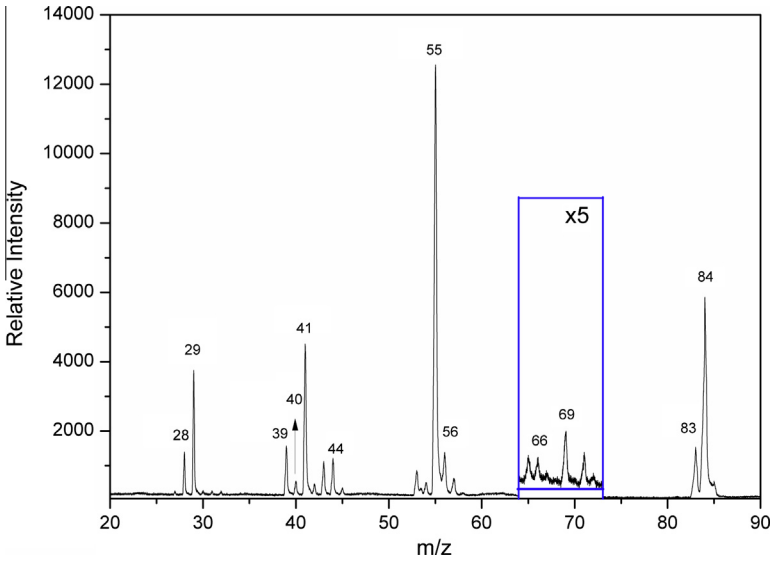

Fig. 1. Photonionization mass spectrum of trans-2-methyl-2-butenal at 15 eV. Peaks 65, 66, 69 and 71 are amplified with a factor of 5.

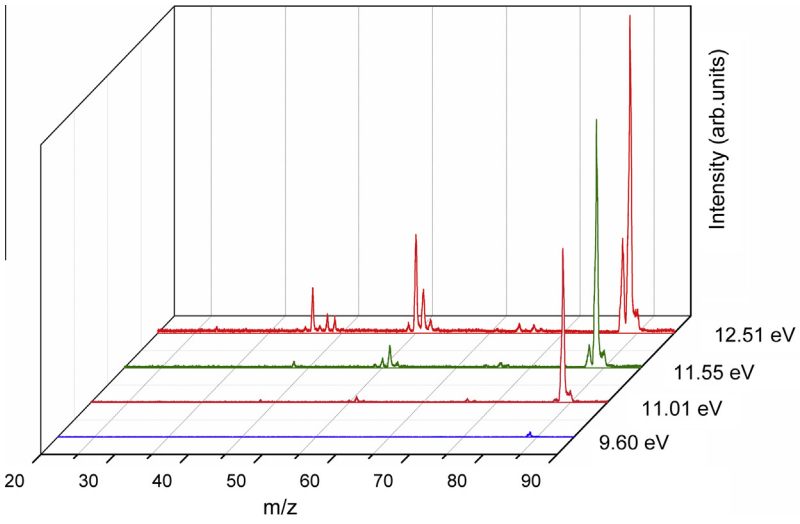

Fig. 2. Photonionization mass spectrum of trans-2-methyl-2-butenal as a function of photon energy.

reported elsewhere [30–32]. AE and IE are defined as the first discernible onset over the linear base line.

In this paper, ionization energy is defined as the amount of energy needed to remove an electron away from neutral gaseous molecule. Theoretical IE of trans-2M2B is calculated as follows:

$$IE(C_5H_8O) = E(C_5H_8O^+ \text{ground state}) - E(C_5H_8O \text{ ground state}) = 9.60 \text{ eV}.$$

From the PIE curve in Fig. 3, experimental IE of parent molecule is assigned to be 9.57 ± 0.03 eV, which is in good agreement of the calculated value and the reported value of 9.60 eV by Masclet and Mouvier [17] in 1978 using photo-electric spectrometry.

Theoretical AE of fragment ions is defined as the amount of energy raise from neutral molecule to the highest energy barrier along the dissociation channel. Dissociation energy (Ed) is calculated by subtracting ionization energy of parent molecule from its appearance energy, Ed = AE − IE. In summary, experimental AEs of $C_5H_7O^+$, $C_4H_5O^+$, $C_4H_8^+$, $C_4H_7^+$, $C_3H_5^+$, $C_3H_4^+$, $C_2H_4^+$, CHO^+, $C_2H_4O^+$ and $C_3H_3^+$ are assigned to be 10.71 ± 0.06, 10.68 ± 0.06, 10.59 ± 0.03, 11.55 ± 0.03, 11.94 ± 0.03, 11.82 ± 0.03, 12.03 ± 0.06, 12.21 ± 0.03, 12.09 ± 0.03 and 12.90 ± 0.03 eV respectively. There are six dissociation channels discussed in our article: $C_5H_7O^+ + H$; $C_4H_5O^+ + CH_3$; $C_5H_6^+ + H_2O$; $C_4H_8^+ + CO \rightarrow (C_3H_5^+ + CH_3 + CO$, $C_3H_4^+ + CH_4 + CO$, $C_2H_4^+ + C_2H_4 + CO$, $C_4H_7^+ + H + CO)$; $C_4H_7^+ + CHO$ $(C_4H_7 + CHO^+)$; and $C_3H_4 + C_2H_4O^+$. Details of the dissociation channels are illustrated in Figs. 5–9. Table 1 lists experimental and theoretical AEs, and Eds. As this is the first work to study the dissociation of trans-2M2B molecule ever to our knowledge, no reported information on AEs of the fragment ions are available. All total energies of species involved in the dissociation procedure are listed in Table 2 as supporting information.

On the first time of being mentioned, products, intermediates and transition states are named with a unique number with the prefix of P (product), INT (intermediate) and TS (transition state) respectively. In the case of isomers, suffix of a, b, c, etc. are applied (for example, P1a in channel1). Geometries of all the involved neutral molecule, parent ion, fragment ions, transition states and intermediates are optimized in CBS-QB3. The results of the optimization of the neutral molecule, parent ion, and the fragment ions are

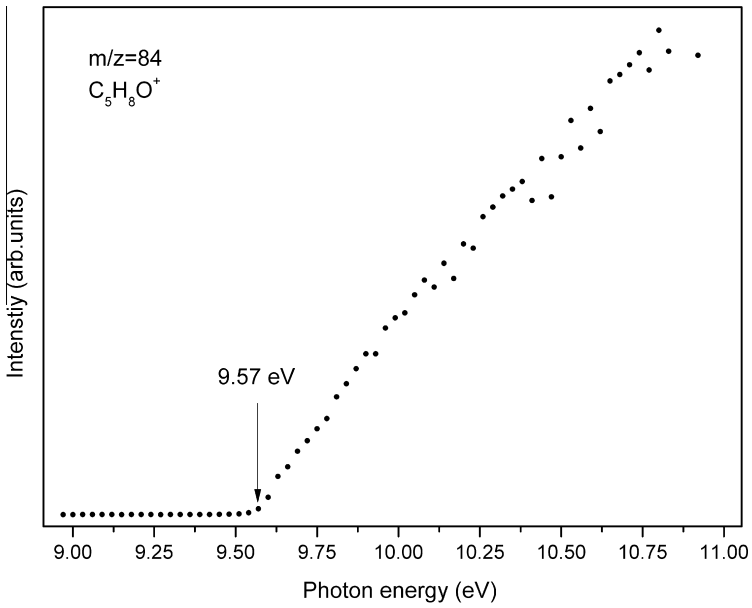

Fig. 3. PIE curve of parent ion $C_5H_8O^+$.

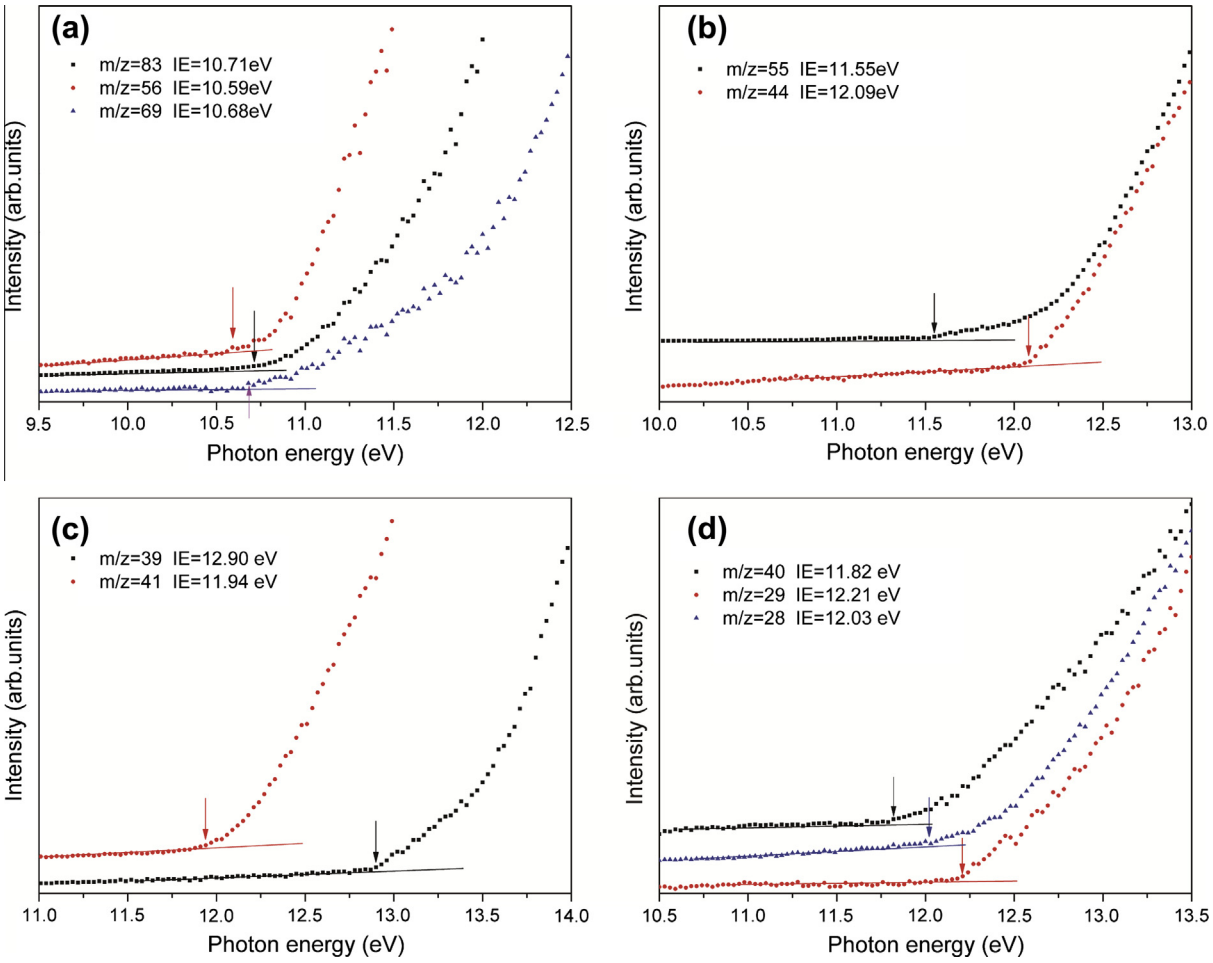

Fig. 4. Normalized PIE curves of fragment ions (a)–(d).

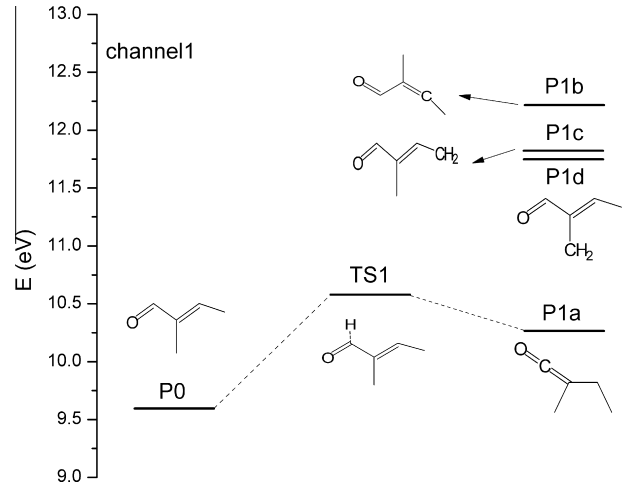

Fig. 5. Details of dissociation channel1. Energy of neutral trans-2-methyl-2-butenal is defined as zero. All the energies of the species are calculated at CBS-QB3 level.

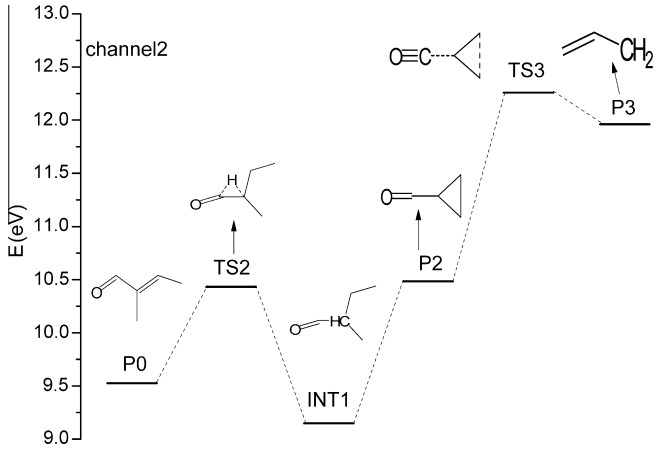

Fig. 6. Details of dissociation channel2. Energy of neutral trans-2-methyl-2-butenal is defined as zero. All the energies of the species are calculated at CBS-QB3 level.

shown in Fig. 10. Geometries of the transition state, intermediates are shown in Fig. 11. The length of bond is in Å unit and the angle is in degrees.

Dissociation mechanisms

Parent ion is formed directly via a VUV single photon ionization procedure (C_5H_8O + photon → $C_5H_8O^+$ + e). When the photon energy goes up, the parent ion undergoes different dissociation procedures. AEs obtained from the PIE curves are compared with the calculated values, and dissociation mechanisms are discussed as below.

Channel1 $C_5H_7O^+ + H$

The H elimination is considered as a one step dissociation process. In the case of t-2M2B, there are four nonequivalent H atoms. We calculated the AEs of four possible fragment ion isomers, and the outcomes are showed in Table 2 and Fig. 5. The experimental AE of $C_5H_7O^+$ (P1, $m/z = 83$) is assigned to be 10.71 ± 0.06 eV (Fig. 4a).

P1a ($[C_5H_7O^+]^a$ in Table 1) is formed from the cleavage of C12–H14 bond, which is 1.106 Å in length. The other three isomers is the H elimination from C2 for P1b, C8 for P1c and C4 for P1d. The C–H bond lengths are 1.089, 1.087 and 1.089 Å correspondingly. Theoretical AEs for P1a, P1b, P1c and P1d are 10.55, 12.21, 11.77 and 11.75 eV. It is not surprising to find that the P1a channel is the lowest energy required. Along the path from parent ion to the product P1a, there is a transition state TS1 with the energy (10.55 eV) about 0.3 eV higher than the products (10.25 eV). We do not deny possible TS for the other three channels, but their AEs are apparently much higher than the experimental values. Since the theoretical result compares well with the experimental value, we tend to consider the H eliminates from the C12. The structure of fragment ion P1a is shown in Fig. 10.

Channel2 $C_4H_5O^+ + CH_3$

Fig. 6 shows the dissociation channel to generates $C_4H_5O^+$ (P2, $m/z = 69$) fragment ion. It is obvious that there are two unequal methyl groups in the parent ion, so we investigated two pathways theoretically and compared with the experimental value 10.68 ± 0.06 eV (Fig. 4a). Direct methyl group elimination is firstly considered but the products are unstable and H shift is unavoidable. To make it more feasible, first, a transition state TS2 is proposed and the H14 transfers from C12 to C1 with an energy barrier of 1.36 eV and INT1 is produced. Second, C–C bond breaks and we scanned the C2–C8 bond length from 1.4 to 4.4 Å. The highest energy is 13.60 eV, which is 2.92 eV higher than the experimental AE value. It is not likely that this channel emerges at lower photon energy.

Taking the rapture of C1–C4 bond, which is 1.55 Å in length, into consideration, we find a more reliable pathway. After the C1–C4 bond directly raptures, one of the three H atoms on the C8 transfers to C2, then, C1 and C8 rebond to form a three-membered ring, P2. In the three-membered ring, C1–C8 and C1–C2 bond are the same in length (1.57 Å) and the C2–C8 bond is slightly shorter (1.47 Å). Calculated AE of this channel is 10.47 eV, in good agreement with the experimental value.

The P2 could dissociate further by losing CO, and produce $C_3H_5^+$ (P3, $m/z = 41$). From the PIE curve, AE of $C_3H_5^+$ is assigned to be 11.94 ± 0.03 eV (Fig. 4c). However, theoretical study shows that there is a TS3 with the energy of 12.26 eV along the dissociation pathway. Considering the tunnel effect, there might be possibility that P3 is generated in this channel, yet there is a lower energy required and thus more feasible pathway for the formation of $C_3H_5^+$ in channel4.

Channel3 $C_5H_6^+ + H_2O$

In the studies on the homologues of t-2M2B, to name but a few, the study on the photondissociation of trans-crotonaldehyde by Shu et al. [22] in 2004, and the dissociation of propenal by Chaudhuri and Lee in 2011 [19], dehydration is always one of the dominant reactions. Their experiments were carried out by applying 193 nm laser and then the neutral parent molecule dissociated. However, in our study, the product of dehydration, $C_5H_6^+$, is so weak in signal that the PIE curve is strongly affected by the base line. We think the reliability of its PIE curve is challenged. Here, we investigate the dissociation pathways theoretically. Four dissociation channels that possibly produce $C_5H_6^+$ (P4, $m/z = 66$) are grouped into two groups according to their final products. Channel3a and channel3b are shown in Fig. 7a, and channel3c and channel3d are shown in Fig. 7b.

In channel3a, first, the C1–C12 bond rotates to form a C2–C1–C12–C13 dihedral angle −3.32°. Second, H3 from C2 transfers to O13 via TS4 to form intermediate INT2. Energy for TS4 is 10.46 eV, which is not high. However, there is a relatively high energy barrier of TS5 (14.01 eV) in the next step that H14 shifts from C12 to O13. We also examined the pathway channel3b that H14 shift from C12 comes first via TS6 and followed by H3 shift from C2 via TS7. Calculated AE for this channel is 13.17 eV, much lower than that of channel3a. The final products are P4a and

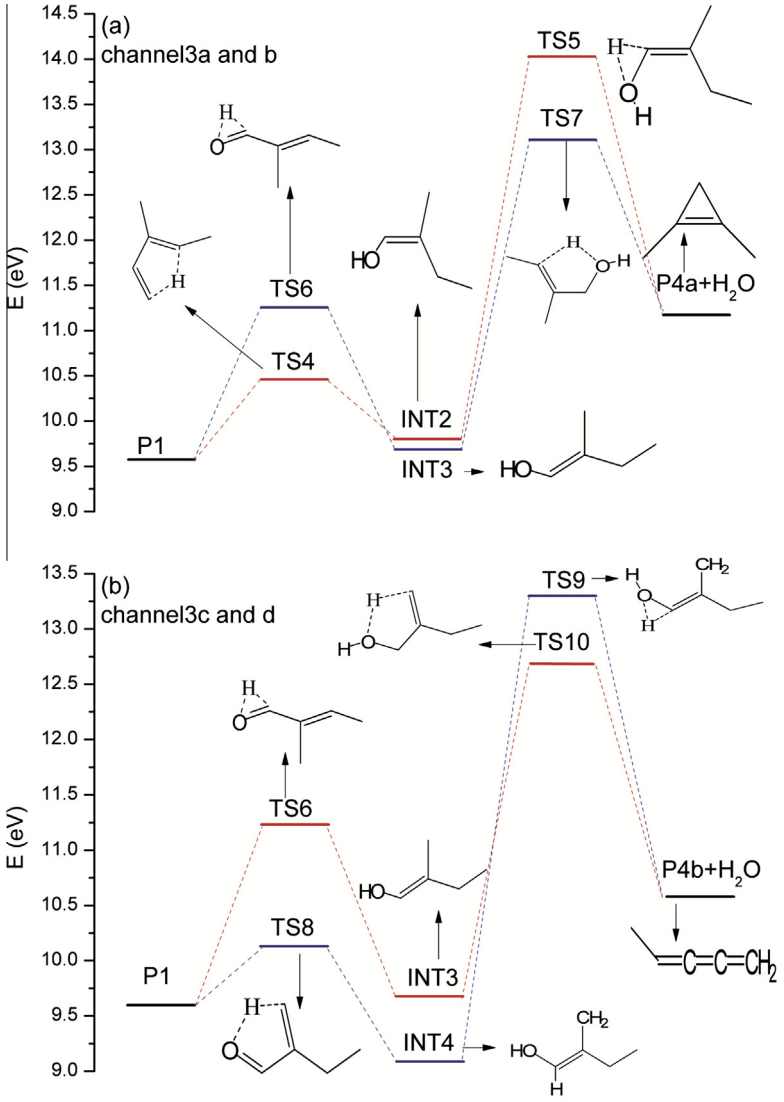

Fig. 7. Details of dissociation channel3 (a)–(d). Energy of neutral trans-2-methyl-2-butenal is defined as zero. All the energies of the species are calculated at CBS-QB3 level.

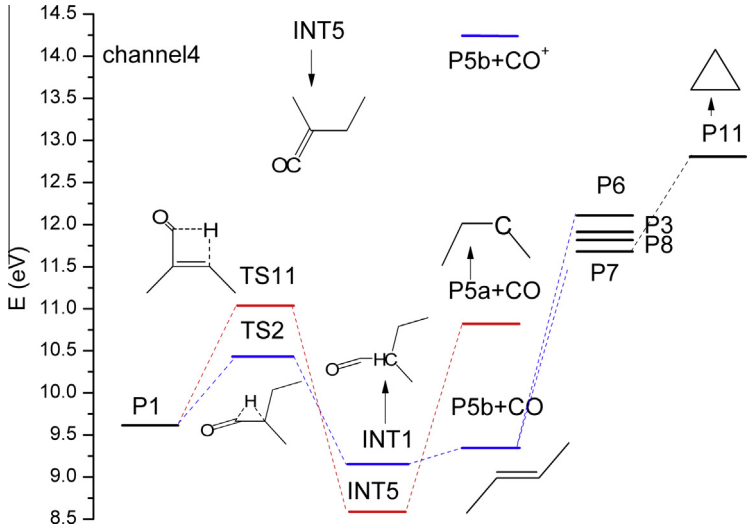

Fig. 8. Details of dissociation channel4. Energy of neutral trans-2-methyl-2-butenal is defined as zero. All the energies of the species are calculated at CBS-QB3 level.

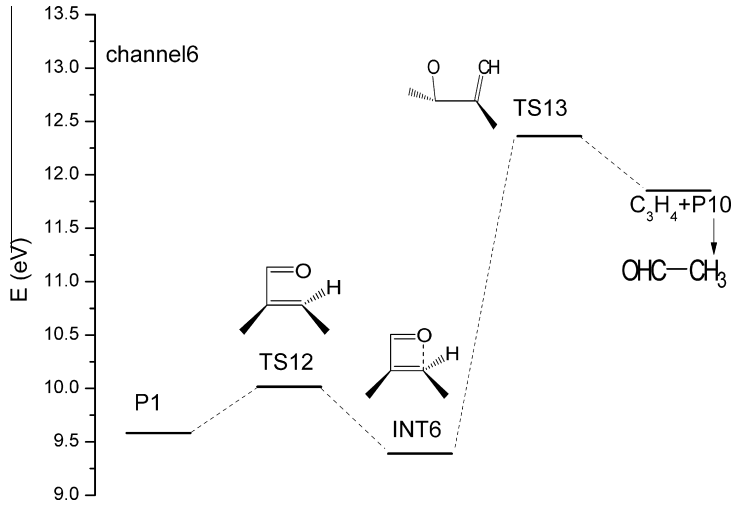

Fig. 9. Details of dissociation channel6. Energy of neutral trans-2-methyl-2-butenal is defined as zero. All the energies of the species are calculated at CBS-QB3 level.

Table 1
Experimental and theoretical IE of the parent molecule. Experimental and theoretical AE and Ed of the fragment ions. Possible dissociation channels.

	Ions	IE or AEs (eV) experimental	IE or AEs (eV) theoretical	Ed (eV) experimental	Ed (eV) theoretical	Possible dissociation channels
P0	$C_5H_8O^+$	9.57 ± 0.03	9.60	–	–	–
P1a	$C_5H_7O^+$	10.71 ± 0.06	10.55	1.14	0.95	$[C_5H_7O^+]^a + H$
P2	$C_4H_5O^+$	10.68 ± 0.06	10.47	1.29	0.87	$C_4H_5O^+ + CH_3$
P3	$C_3H_5^+$	11.94 ± 0.03	11.93	2.37	2.33	$C_4H_8^+ \rightarrow C_3H_5^+ + CH_3$
P4b	$C_5H_6^+$	–	12.69	–	3.09	$[C_5H_6^+]^b + H_2O$
P5	$C_4H_8^+$	10.59 ± 0.03	10.45	1.02	0.85	$C_4H_8^+ + CO$
P6a	$C_4H_7^+$	11.55 ± 0.03	11.49	1.98	1.89	$C_4H_8^+ \rightarrow [C_4H_7^+]^a + H$
P7	$C_3H_4^+$	11.82 ± 0.03	11.71	2.25	2.11	$C_4H_8^+ \rightarrow C_3H_4^+ + CH_4$
P8	$C_2H_4^+$	12.03 ± 0.06	11.84	2.46	2.24	$C_4H_8^+ \rightarrow C_2H_4^+ + C_2H_4$
P9+	CHO^+	12.21 ± 0.03	12.32	2.64	2.72	$C_4H_7 + CHO^+$
P10	$C_2H_4O^+$	12.09 ± 0.03	12.34	2.52	2.74	$C_2H_4O^+ + C_3H_4$
P11	$C_3H_3^+$	12.90 ± 0.03	12.79	3.33	3.19	$C_3H_4^+ \rightarrow C_3H_3^+ + H$

H_2O. In channel3c, C12–C1–C4–H6–O13 form a five-membered ring in TS8. The H6 transfers to O13 to form INT4. Then, as in the case of channel3a, the H1 shifts to O13 via TS9 of 13.29 eV. Channel3d has the lowest AE. First, H14 transfers from C12 to O13 via TS6, which is also involved in channel3b. Then C12–C1–C4–H6–O13 form a slightly twisted five-membered ring in TS10. Dihedral angle of the O13–C12–C1–C4 is −21.18°. H6 atom is 1.16 Å from O13 and 1.59 Å from C4. Finally, the H_2O is eliminated from the rearranged parent ion and P4b ($[C_5H_6^+]^b$ in Table 1) is generated. The theoretical AE in this dissociation pathway is 12.69 eV. Methyl group on α carbon is involved in the isomerization of parent ion in channel3c and 3d.

Channel4 $C_4H_8^+ + CO \rightarrow (C_3H_5^+ + CH_3 + CO,\ C_3H_4^+ + CH_4 + CO,\ C_2H_4^+ + C_2H_4 + CO,\ C_4H_7^+ + H + CO)$

$C_4H_8^+$ (P5, $m/z = 56$) is the product of the elimination of CO. Experimental AE of P5 is 10.59 ± 0.03 eV (Fig. 4a). For propenal and trans-crotonaldehyde, Elimination of CO is one of the major dissociation pathways. However, Peak of P5 is just a medium peak in our mass spectra, not as strong as in the case of the former two adldehydes.

H shift from C12 is necessary before CO elimination, and there are two pathways. In channel4a, H14 transfers from C12 to C2. First, rotation of C1–C2 bond exposes C2 to H14. Second, H14 transfers from C12 to C2 via a four-memberd ring C12–C1–C2–H14 in TS11. Dihedral angle of C12–C1–C2–C8 is 133.84° in TS11. Theoretical AE of this channel is 11.01 eV, and it is 0.42 eV more than the experimental AE. In another pathway, channel4b, H14 from C12 transfers to C1 via TS2 (AE = 10.45 eV), which is 0.14 eV lower than the experimental AE. After the H14 shift, direct cleavage of C12–C1 bond release CO and produce $C_4H_8^+$. $C_4H_8^+$ in channel4a is P5a (10.72 eV), 1.41 eV more than P5b in channel4b. Channel4b has a lower AE and it is more feasible than channel4a theoretically.

Peak at $m/z = 28$ is initially assumed to be CO^+. However, the calculation shows that the lowest AE for CO^+ was 14.24 eV via channel $C_5H_8O^+ \rightarrow C_4H_8 + CO^+$, which is still much higher than the experimental AE value. The possible generation of peak at $m/z = 28$ is the further dissociation of $C_4H_8^+$, which had been well studied experimentally and theoretically by Hudson et al. [33–35]. Their work pointed out that $C_4H_8^+$ will dissociate mainly via four reactions: $C_4H_8^+ \rightarrow C_4H_7^+ + H$; $C_4H_8^+ \rightarrow C_3H_5^+ + CH_3$; $C_4H_8^+ \rightarrow C_3H_4^+ + CH_4$; $C_4H_8^+ \rightarrow C_2H_4^+ + C_2H_4$. In the dissociation procedure, H atom and/or methyl group shift take place before elimination. We are not interested in retelling the dissociation mechanism in their works, and the results of our work are as follows: peaks at $m/z = 55$, 41, 40 and 28 are assigned to be $C_4H_7^+$ (P6), $C_3H_5^+$ (P3), $C_3H_4^+$ (P7) and $C_2H_4^+$ (P8), and theoretical AEs are 11.38, 11.93, 11.71 and 11.84 eV respectively. The experimental values are 11.55 ± 0.03 (Fig. 4b), 11.94 ± 0.03 (Fig. 4c), 11.82 ± 0.03 (Fig. 4d) and 12.03 ± 0.06 eV (Fig. 4d) correspondingly. Theoretical and experimental values match well with each other except P6. As in the case of P6, H elimination from unequivalent C atoms in P5 generates the P6a and P6b (see in Fig. 10). However, as the peak

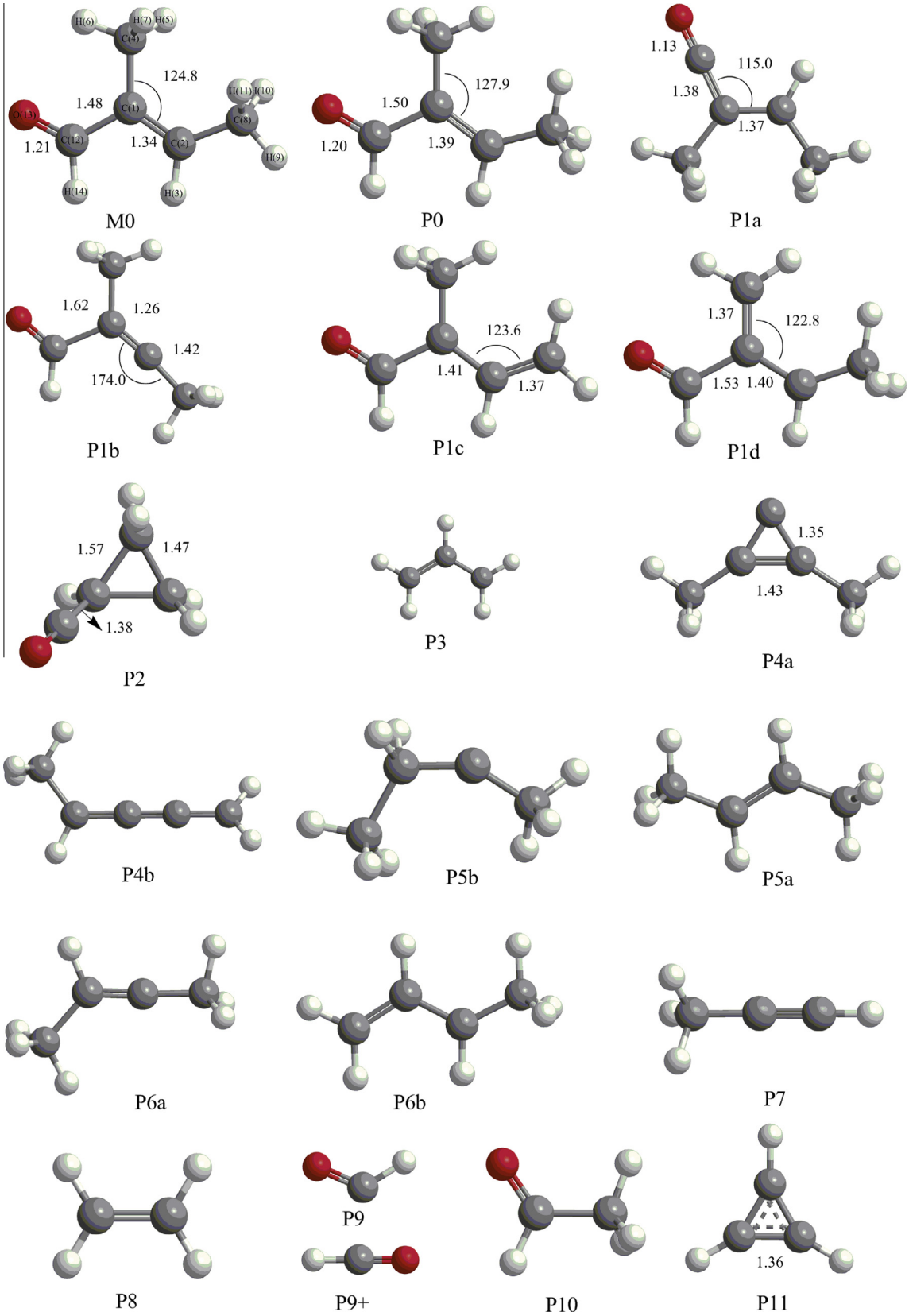

Fig. 10. Geometries of related products optimized with CBS-QB3.

of $m/z = 55$ is the strongest, we tend to believe that fragment $C_4H_7^+$ is mainly produced by direct dissociation channel5 rather than the dissociation of $C_4H_8^+$. Peak $m/z = 39$, assigned to be $C_3H_3^+$ (P11, $m/z = 39$), is a medium peak. The $C_3H_4^+$ cation undergoes further dissociation to generate $C_3H_3^+$. A lot of lab and theoretical work have been done on the dissociation mechanism of propyne cation

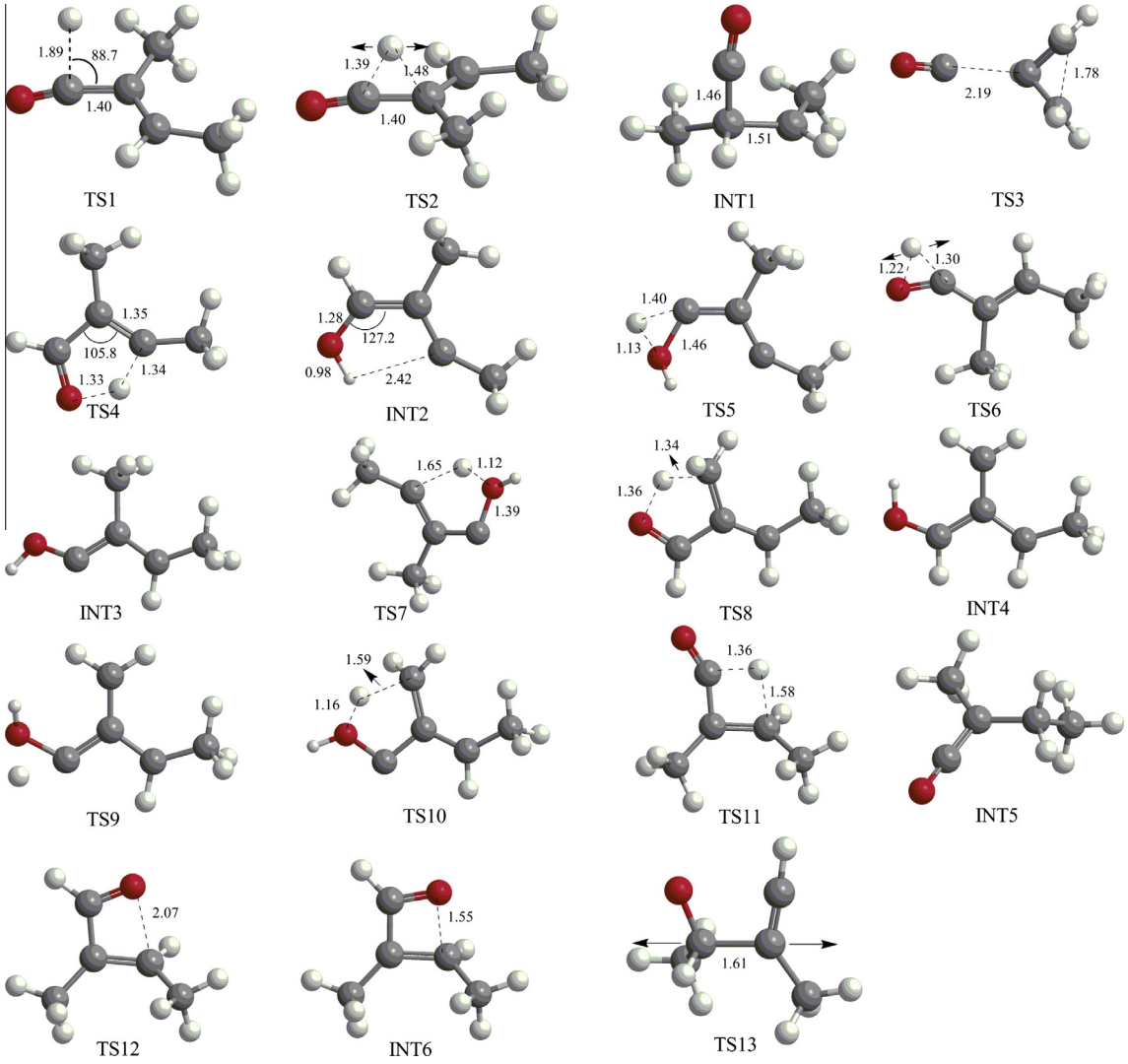

Fig. 11. Geometries of transition states and intermediates obtained with CBS-QB3.

[36,37]. Here, we deliver our result in brief. A three-membered ring is formed and $C_3H_3^+$ is of the lowest energy in this conformation as shown in Fig. 10. The experimental AE for $C_3H_3^+$ is 12.90 ± 0.03 eV (Fig. 4c), and theoretical AE is 12.79 eV.

Channel5 $C_4H_7^+ + CHO$ ($C_4H_7 + CHO^+$)

$C_4H_7^+$ (P6a,[$C_4H_7^+$]^a in Table1) and CHO^+ (P9+, m/z = 29) could be generated via the direct cleavage of C1–C12 bond. As no rearrangement is involved, a dissociation channel illustration is dispensable here. Li and Baer studied the dissociation of the acrolein ions theoretically in 2002 [38]. In their work, a ion–dipole complex between HCO^+ and C_2H_3, or HCO and $C_2H_3^+$ is reported at the MP2/6-31G* level. It also gives a hint here on the charge switch of CHO^+ and C_4H_7 or CHO and $C_4H_7^+$. From the PIE curves, experimental AEs for CHO^+ and $C_4H_7^+$ are 12.21 ± 0.03 (Fig. 4d) and 11.55 ± 0.03 eV (Fig. 4b), respectively. According to our computational work, the theoretical AEs for CHO^+ and $C_4H_7^+$ are 12.32 and 11.49 eV respectively, which agree well with the experimental ones.

Channel6 $C_3H_4 + C_2H_4O^+$

Peak m/z = 44, representing $C_2H_4O^+$ (P10, m/z = 44), is a medium peak in the mass spectra at 15 eV. It is not that outstanding in EI mass spectrum from NIST. Experimental AE is 12.09 ± 0.03 eV (Fig. 4b) for $C_2H_4O^+$. With the aid of theoretical calculation, the dissociation mechanism is described as bellow. First, C12–C1 and C1–C2 bonds rotate to change the conformation of parent ion, and expose O13 to C2. Second, intermediate INT6 is generated via transition state TS12. The dihedral angle of C2–C1–C12–O13 in TS12 is −14.47° and that of H3–C1–C2–C8 is 165.65°. In INT6 C12–C1–C2–O13 forms a four-membered ring with a weak bond (1.55 Å) between C2 and O13. Third, resonance structure of INT6, with a relatively strong bond connecting O13–C2 and C12–C1 yet weak bond between O13–C12, relax the C1–C2 bond until it raptures via TS13 and fragment ion P10 is formed. P7 could be produced in this channel, $C_3H_4^+ + C_2H_4O$. Considering TS13, theoretical AE for P7 in this channel is no less than 12.34 eV, 0.63 eV higher than that in channel4 which is more feasible.

Conclusion

Dissociative photoionization of trans-2-methyl-2-butenal was carried out with supersonic expansion technology and photoionization mass spectrometry. By scanning the photon energy in 0.03 eV step, the ionization energy of trans-2-methyl-2-butenal and the appearance energies of major fragment ions $C_5H_7O^+$, $C_4H_5O^+$, $C_4H_8^+$, $C_4H_7^+$, $C_3H_5^+$, $C_3H_4^+$, $C_2H_4^+$, CHO^+, $C_2H_4O^+$ and $C_3H_3^+$ are obtained. All the geometries and energies of the fragments,

intermediates and transition states involved in the dissociations are obtained at CBS-QB3 level. The theoretical IE and AEs are in good agreement with experimental ones. On comparison of theoretical and experimental results, the mechanisms of the dissociation pathways are discussed. Methyl group on α carbon is involved in the isomerization and dissociation process. This work is helpful to the investigation on the unique role of t-2M2B in the secondary organic aerosol formation procedure via atmospheric chemistry reactions.

Acknowledgements

This work has been supported by the National Natural Science of China (Nos. 11075165, U1232209, 11275006, U1232130, 41275127 and 10979048). The authors would like to thank the Supercomputing Center of University of Science and Technology of China.

Appendix A. Supplementary material

Supplementary data associated with this article can be found, in the online version, at http://dx.doi.org/10.1016/j.molstruc.2014.03.021.

References

[1] J. Wildt, K. Kobel, G. Schuh-Thomas, A.C. Heiden, J. Atmos. Chem. 45 (2003) 173.
[2] R. Atkinson, J. Arey, Atmos. Environ. 37 (2003) S197.
[3] R. Atkinson, J. Arey, Chem. Rev. 103 (2003) 4605.
[4] D. Grosjean, E. Grosjean, A.W. Gertler, Environ. Sci. Technol. 35 (2001) 45.
[5] W. Kirstine, I. Galbally, Y.R. Ye, M. Hooper, J. Geophys. Res.-Atmos. 103 (1998) 10605.
[6] S. Owen, C. Boissard, R.A. Street, S.C. Duckham, O. Csiky, C.N. Hewitt, Atmos. Environ. 31 (1997) 101.
[7] S.E. Paulson, R.C. Flagan, J.H. Seinfeld, Int. J. Chem. Kinet. 24 (1992) 79.
[8] T. Karl, R. Fall, P.J. Crutzen, A. Jordan, W. Lindinger, Geophys. Res. Lett. 28 (2001) 507.
[9] R. Fall, T. Karl, A. Jordon, W. Lindinger, Atmos. Environ. 35 (2001) 3905.
[10] M.S. Jang, N.M. Czoschke, S. Lee, R.M. Kamens, Science 298 (2002) 814.
[11] A.W.H. Chan, M.N. Chan, J.D. Surratt, P.S. Chhabra, C.L. Loza, J.D. Crounse, L.D. Yee, R.C. Flagan, P.O. Wennberg, J.H. Seinfeld, Atmos. Chem. Phys. 10 (2010) 7169.
[12] I. Magneron, R. Thevenet, A. Mellouki, G. Le Bras, G.K. Moortgat, K. Wirtz, J. Phys. Chem. A 106 (2002) 2526.
[13] E.C. Tuazon, S.M. Aschmann, N. Nishino, J. Arey, R. Atkinson, Phys. Chem. Chem. Phys. 7 (2005) 2298.
[14] G. Fantechi, N.R. Jensen, J. Hjorth, J. Peeters, Int. J. Chem. Kinet. 30 (1998) 589.
[15] K. Sato, B. Klotz, T. Taketsugu, T. Takayanagi, Phys. Chem. Chem. Phys. 6 (2004) 3969.
[16] B.J. Finlayson-Pitts Jr., J.N.P. Chemistry of the Upper and lower Atmosphere: theory, Experiments, and Applications 2000.
[17] P. Masclet, G. Mouvier, J. Electron. Spectrosc. 14 (1978) 77.
[18] C.H. Chin, S.H. Lee, J. Chem. Phys. (2011) 134.
[19] C. Chaudhuri, S.H. Lee, Phys. Chem. Chem. Phys. 13 (2011) 7312.
[20] W.H. Fang, J. Am. Chem. Soc. 121 (1999) 8376.
[21] B.M. Haas, T.K. Minton, P. Felder, J.R. Huber, J. Phys. Chem.-Us 95 (1991) 5149.
[22] J.N. Shu, D.S. Peterka, S.R. Leone, M. Ahmed, J. Phys. Chem. A 108 (2004) 7895.
[23] S.S. Wang, R.H. Kong, X.B. Shan, Y.W. Zhang, L.S. Sheng, Z.Y. Wang, L.Q. Hao, S.K. Zhou, J. Synchrotron Radiat. 13 (2006) 415.
[24] S.H. Zhou, G.B. Chu, L.L. Cao, X.B. Shan, F.Y. Liu, J.G. Han, L.S. Sheng, Eur. J. Mass Spectrom. 17 (2011) 101.
[25] W.Z. Fang, L. Gong, Q. Zhang, X.B. Shan, F.Y. Liu, Z.Y. Wang, L.S. Sheng, J. Chem. Phys. (2011) 134.
[26] Q. Zhang, W.Z. Fang, Y. Xie, M.Q. Cao, Y.J. Zhao, X.B. Shan, F.Y. Liu, Z.Y. Wang, L.S. Sheng, J. Mol. Struct. 1020 (2012) 105.
[27] J.A. Montgomery, M.J. Frisch, J.W. Ochterski, G.A. Petersson, J. Chem. Phys. 112 (2000) 6532.
[28] J.A. Montgomery, M.J. Frisch, J.W. Ochterski, G.A. Petersson, J. Chem. Phys. 110 (1999) 2822.
[29] M.J. Frisch, G.W.T., H.B. Schlegel, G.E. Scuseria, M.A. Robb, J.R.C., G. Scalmani, V. Barone, B. Mennucci, G.A. Petersson, H.N., M. Caricato, X. Li, H.P. Hratchian, A.F. Izmaylov, J.B., G. Zheng, J.L. Sonnenberg, M. Hada, M. Ehara, K.T., R. Fukuda, J. Hasegawa, M. Ishida, T. Nakajima, Y. Honda, O.K., H. Nakai, T. Vreven, J.A. Montgomery, Jr., J.E. Peralta, F.O., M. Bearpark, J.J. Heyd, E. Brothers, K.N. Kudin, V.N.S., T. Keith, R. Kobayashi, J. Normand, K. Raghavachari, A.R., J.C. Burant, S.S. Iyengar, J. Tomasi, M. Cossi, N.R., J.M. Millam, M. Klene, J.E. Knox, J.B. Cross, V. Bakken, C.A., J. Jaramillo, R. Gomperts, R.E. Stratmann, O. Yazyev, A.J.A., R. Cammi, C. Pomelli, J.W. Ochterski, R.L. Martin, K.M., V.G. Zakrzewski, G.A. Voth, P. Salvador, J.J. D., S. Dapprich, A.D. Daniels, O. Farkas, J.B.F., J.V. Ortiz, J. Cioslowski, D.J. Fox, G. Inc, Wallingford CT, 2010.
[30] K.R. Wilson, M. Jimenez-Cruz, C. Nicolas, L. Belau, S.R. Leone, M. Ahmed, J. Phys. Chem. A 110 (2006) 2106.
[31] K.R. Wilson, L. Belau, C. Nicolas, M. Jimenez-Cruz, S.R. Leone, M. Ahmed, Int. J. Mass Spectrom. 249 (2006) 155.
[32] S.Y. Chiang, M. Bahou, K. Sankaran, Y.P. Lee, H.F. Lu, M.D. Su, J. Chem. Phys. 118 (2003) 62.
[33] C.E. Hudson, D. Wang, D.J. McAdoo, Int. J. Mass Spectrom. 236 (2004) 105.
[34] J.A. Booze, M. Schweinsberg, T. Baer, J. Chem. Phys. 99 (1993) 4441.
[35] W.J. Chesnavich, L. Bass, T. Su, M.T. Bowers, J. Chem. Phys. 74 (1981) 2228.
[36] B.T. Psciuk, P. Tao, H.B. Schlegel, J. Phys. Chem. A 114 (2010) 7653.
[37] C.S. Matthews, P. Warneck, J. Chem. Phys. 51 (1969) 854.
[38] Y. Li, T. Baer, Int. J. Mass Spectrom. 218 (2002) 19.